Original article

MOLECULAR METABOLISM

Triggering the adaptive immune system with commensal gut bacteria protects against insulin resistance and dysglycemia

Céline Pomié [1,2], Vincent Blasco-Baque [1,2], Pascale Klopp [1,2], Simon Nicolas [1,2], Aurélie Waget [1,2], Pascale Loubières [1,2], Vincent Azalbert [1,2], Anthony Puel [1,2], Frédéric Lopez [4], Cédric Dray [5], Philippe Valet [5], Benjamin Lelouvier [3], Florence Servant [3], Michael Courtney [3], Jacques Amar [1,2], Rémy Burcelin [1,2,*], Lucile Garidou [1,2,**]

ABSTRACT

Objective: To demonstrate that glycemia and insulin resistance are controlled by a mechanism involving the adaptive immune system and gut microbiota crosstalk.

Methods: We triggered the immune system with microbial extracts specifically from the intestinal ileum contents of HFD-diabetic mice by the process of immunization. 35 days later, immunized mice were fed a HFD for up to two months in order to challenge the development of metabolic features. The immune responses were quantified. Eventually, adoptive transfer of immune cells from the microbiota-immunized mice to naïve mice was performed to demonstrate the causality of the microbiota-stimulated adaptive immune system on the development of metabolic disease. The gut microbiota of the immunized HFD-fed mice was characterized in order to demonstrate whether the manipulation of the microbiota to immune system interaction reverses the causal deleterious effect of gut microbiota dysbiosis on metabolic disease.

Results: Subcutaneous injection (immunization procedure) of ileum microbial extracts prevented hyperglycemia and insulin resistance in a dose-dependent manner in response to a HFD. The immunization enhanced the proliferation of CD4 and CD8 T cells in lymphoid organs, also increased cytokine production and antibody secretion. As a mechanism explaining the metabolic improvement, the immunization procedure reversed gut microbiota dysbiosis. Finally, adoptive transfer of immune cells from immunized mice improved metabolic features in response to HFD.

Conclusions: Glycemia and insulin sensitivity can be regulated by triggering the adaptive immunity to microbiota interaction. This reduces the gut microbiota dysbiosis induced by a fat-enriched diet.

Keywords Gut microbiota and metabolic diseases; Immunity; Insulin resistance

1. INTRODUCTION

Trillions of bacteria inhabit our gut establishing a stable ecology and symbiosis with the host. The last decade demonstrated that changes in this ecology characterize metabolic disease [1]. This dysbiosis was reversible since diet-induced body weight loss restored a healthy gut microbiota ecology further suggesting its causal role [2,3]. The causality of gut microbiota during the development of metabolic disease was demonstrated in rodents by showing that the obesity phenotype could be transferred from obese mice to germ free recipient mice by colonizing the latter with the cecal or ileal microbiota from the former [4,5]. It was also shown that hepatic steatosis [6], atherosclerosis [7] as well as the therapeutic effect of bariatric surgery on obesity [8] and the deleterious effect of dietary lipids [9] were under the control, at least in part, of the gut microbiota. Although the causal role of gut microbiota in the control of metabolic disease is commonly accepted, the identification of the corresponding mechanisms is in its infancy. An important leading concept is that gut microbiota ecology regulates the

[1]Institut National de la Santé et de la Recherche Médicale (INSERM), Toulouse, France [2]Université Paul Sabatier (UPS), Unité Mixte de Recherche (UMR) 1048, Institut des Maladies Métaboliques et Cardiovasculaires (I2MC), Team 2: « Intestinal Risk Factors, Diabetes, Dyslipidemia », 1 avenue Jean Poulhès, BP 84225, F-31432 Toulouse Cedex 4, France [3]VAIOMER SAS, 516 Rue Pierre et Marie Curie, 31670 Labège, France [4]Groupe Protéomique Centre Recherche Cancer Toulouse, Université Paul Sabatier (UPS), Unité Mixte de Recherche (UMR) 1037, 2 avenue Hubert Curien, CS 53717, 31037 Toulouse Cedex 1, France [5]Université Paul Sabatier (UPS), Unité Mixte de Recherche (UMR) 1048, Institut des Maladies Métaboliques et Cardiovasculaires (I2MC), Team 3: « Adipokines, obesity and associated Pathologies », 1 avenue Jean Poulhès, BP 84225, F-31432 Toulouse Cedex 4, France

*Corresponding author. INSERM UMR1048-I2MC, Team 2 "Intestinal Risk Factors, Diabetes and Dyslipidemia", 1 avenue Jean Poulhès, BP84225, F-31432 Toulouse Cedex 4, France. Tel. +33 561 325 614; fax: +33 5 31 22 41 36. E-mail: remy.burcelin@inserm.fr (R. Burcelin).

**Corresponding author. INSERM UMR1048-I2MC, Team 2 "Intestinal Risk Factors, Diabetes and Dyslipidemia", 1 avenue Jean Poulhès, BP84225, F-31432 Toulouse Cedex 4, France. Tel. +33 561 325 614; fax: +33 5 31 22 41 36. E-mail: lucile.garidou@gmail.com (L. Garidou).

Abbreviations: AT, Adipose tissue; APC, Antigen presenting cells; LN, Lymph nodes; NC, Normal chow; T2D, Type 2 diabetes; VL, Vastus lateralis muscle

Received February 26, 2016 • Revision received March 17, 2016 • Accepted March 22, 2016 • Available online 28 March 2016

http://dx.doi.org/10.1016/j.molmet.2016.03.004

innate and adaptive immune systems at birth [10,11]. Commensal bacteria, such as segmented filamentous bacteria, favor the development of Th17 cells in the gut of rodents [12,13], and *Clostridium* and *Bacteroides fragilis* favor the development of Tregs through mechanisms involving, at least in part, butyrate production from dietary fiber fermentation [14,15]. Alternatively, commensal bacteria overgrowth is under the control of the host immune system, specifically IgAs. These antibodies maintain intestinal vigilance [16] and shape gut microbiota [17]. Consequently, mutations in the immune system are associated with changes in gut microbiota ecology that increase susceptibility to pathologies [18,19]. As an example in the context of metabolic disease, the genetic ablation of the TLR2 gene in mice induced obesity and insulin resistance through modulation of gut microbiota [20]. Importantly, the ecology of gut microbiota varies according to the intestinal segments notably upon the gradient of oxygen, pH, or bile acids [21]. Furthermore, the luminal, mucosal, and cryptic microbiota are different, calling into question the importance of the local dysbiosis. Therefore, the role played by gut microbiota in the control of metabolic disease could depend on a local dysbiosis. Similarly, the intestinal immune system varies according to the intestinal segment [16], and the bacteria interacting with the immune system could be distributed locally rather than widely throughout the gut. Therefore, along the same line of investigation we recently showed that an impaired intestinal defense was characterized by a reduction of the number and frequency of IL17-producing CD4 T cells in the *lamina propria* of the ileum while little or no change was observed in the colon [5].

Thus, the crosstalk between the immune system and gut microbiota localized to the ileum could be crucial in the development of metabolic disease. To address this question, we challenged the immune system with gut ileum microbiota extracts from diabetic mice by an immunization procedure and investigated whether it improved metabolic disease by challenging the mice with a high-fat diet (HFD). The immunization prevents HFD-induced insulin resistance and dysglycemia. The impact on the metabolic features was linked to a mechanism controlling gut microbiota dysbiosis, suggesting that vaccination may be considered as a possible therapeutic approach for T2D.

2. MATERIALS AND METHODS

2.1. Animal models

Eight-week-old C57Bl6/J and CD45.1 C57Bl6/J male mice were purchased from Charles River and maintained at the Inserm Toulouse animal facilities. Rag1-deficient mice were bred in the Inserm Toulouse animal facility. Mice were fed a normal chow diet containing 83.9% cereals, 12% protein, 4.1% vitamin and mineral mixture (Safe, R04) or a HFD containing 72% fat (corn oil, lard), 28% protein, $<1\%$ carbohydrate (Safe). This animal model is intended for studying the impact of a fat-enriched diet independent of obesity. The high content in fat and the absence of carbohydrate favor a rapid hyperglycemia without body weight gain, as described previously [5,22,23]. These mice are moderately insulin resistant, which may be linked to the short duration of the treatment (one month). The HFD is highly lipotoxic and hampers glucose-induced insulin secretion leading to low insulin secretion rates and to hyperglycemia. Linked to the low insulin levels, the body weight of the 70% fat-enriched diet fed mice remains low and could be considered as a MODY like type of model. As an example GK (Goto Kakizaki) rats are largely used in the literature and are lean with low plasma insulin levels. Hence, this diet is a useful tool for studying the impact of a therapeutic strategy on hyperglycemia without the confounding of improved fat mass. All mice were housed under specific pathogen-free conditions. The ethics committee of Rangueil Hospital approved the experiments.

2.2. Immunization of mice

Ten cm-long segments of ileum (up to the cecum) were dissected from mice fed a HFD for 4 weeks. Luminal intestinal contents were collected, suspended in PBS and debris was removed. The supernatant was sonicated (Branson Sonifier 150, Branson Ultrasonics) and diluted in PBS before subcutaneous injection (200 μl). Intestinal extracts were also prepared from mice treated with 1.0 g/l ampicillin and 0.5 g/l neomycin (Sigma) in their drinking water for 4 weeks [24].

2.3. Metabolic parameter monitoring

For the intraperitoneal glucose tolerance test (IPGTT), mice were fasted for 6 h then injected with glucose (1 g/kg, 20% glucose). Glycemia in blood samples collected from the tail vein was determined by means of a glucose meter (Roche Diagnostics). The glycemic index is the sum of the glycemic values multiplied by the duration of the test. Plasma insulin concentration was determined by ELISA (Mercodia Kit) according to the manufacturer's instructions on blood samples collected 30 min before and 15 min after the glucose load. Euglycemic hyperinsulinemic clamping was performed as described previously [25]. Briefly, the mice were fasted for 6 h and then infused at a rate of 18 mU kg^{-1} min^{-1} of insulin for 3 h. Simultaneously, a 20% glucose solution was infused to maintain a steady glycemia while a continuous ^{3}H-glucose was performed to assess the glucose turnover rate. Body mass composition was analyzed by quantitative nuclear magnetic resonance using an EchoMRI-100TM.

2.4. Liver leukocyte isolation

Infiltrating leukocytes were isolated from livers as previously described [26]. Briefly, livers were infused with Liberase (Roche) and incubated for 30 min at 37 °C. Single-cell suspensions were prepared by mechanically disrupting the infused tissue by passing it through a 100 μm filter and then centrifuged. Cells were resuspended in 35% Percoll (Amersham Biosciences). The mononuclear cells were extracted, washed and resuspended in PBS. The number of mononuclear cells was determined.

2.5. Intestinal leukocyte isolation

Small intestine segments (20 cm before the cecum) were harvested, cut into 4 segments (5 cm) and Peyer's patches were dissected out from the intestinal segments. The intestinal segments were incubated in RPMI (Life Technologies) supplemented with EDTA (2 mM, Sigma) three times during 20 min at 37 °C. Segments were then washed with RPMI. Subsequently, the intestinal fragments were incubated in RPMI containing collagenase VIII (0.15 mg/ml; Sigma) and DNase I (40 U/ml; Roche) to isolate *lamina propria* leukocytes. Then leukocytes were isolated through a Percoll gradient (GE Healthcare). The leukocytes were then harvested from the 70%–40% Percoll interface, washed in RPMI and suspended in cell culture medium [5]. The number of mononuclear cells was determined and used to calculate the absolute number.

2.6. Adoptive transfer

Splenocytes from CD45.1 mice were harvested 35 days after immunization and 3×10^{7} cells were injected into the peritoneal cavity of mice fed a HFD for 3 days.

2.7. Flow cytometry

Mononuclear cell suspensions were incubated for 15 min with anti-CD16/32 and with antibodies (see below) for 30 min on ice. Dead cells were removed from the analysis using the LIVE/DEAD Fixable Cell Stain Kit (Life Technologies). All data were acquired using a digital flow cytometer (LSR II Fortessa, Becton Dickinson) and analyzed with FlowJo software (Tree Star). Antibodies used were: anti-CD4 eFluor 780 (RMA4-5, eBioscience); anti-CD8 V450 (53.6.7, BD Bioscience); anti-CD45.1 PE-Cy7 (A20, eBioscience); anti-CD45 V500 (30F11, BD Bioscience); anti-CD19 FITC (1D3, BD Bioscience); anti-MHCII FITC (M5/114, BD Bioscience), and anti-TCR PerCP-Cy5.5 (H57, eBioscience). For Foxp3 analysis, cells were fixed, permeabilized with Transcription Factor Staining Buffer (eBioscience) and labeled with monoclonal antibodies against the transcription factor Foxp3 (anti-Foxp3 PE, FJK-16s, eBioscience).

For intracellular cytokine analysis, immune cells were stimulated as previously described [27]. Briefly, cells were incubated for 4 h with 2.5 μg/ml phorbol 12-myristate 13-acetate (PMA), 0.5 μg/ml ionomycin and 2.5 μg/ml brefeldin A (Sigma). The cell surface was stained as described above. The cells were then fixed, permeabilized by using the BD Cytofix/Cytoperm kit (BD Bioscience) and labeled with antibodies against cytokines: anti-IFNγ (XMG1.2), anti-TNFα (MP6-XT22), anti-IL17 (eBio 17B7), and anti-IL4 (11B11) from eBioscience. The isotype-specific control antibodies were used to measure non-specific background staining.

2.8. In vitro proliferation assay

Spleens and lymph nodes were harvested, and cell suspensions were labeled with carboxyfluorescein succinimidyl ester (CFSE; Sigma) to monitor cell division [26]. Cells were stimulated with plate-bound anti-CD3 and anti-CD28 (3 μg/ml and 1.5 μg/ml, respectively). Three days later, cells were harvested, stained with anti-CD4 and anti-CD8 and analyzed by flow cytometry.

2.9. Plasma immunoglobulin concentration

The immunoglobulin concentration in plasma was quantified by multiplex ELISA using the MILLIPLEX MAP Mouse Immunoglobulin Isotyping Kit (Millipore) according to the manufacturer's protocol. The assays were analyzed by using a Luminex 100 IS analyzer and xMAP technology (Luminex Corporation).

2.10. Western blot analysis

Muscle and liver samples were lysed, and the proteins were separated by SDS polyacrylamide gel electrophoresis on 4–12% Criterion XT gels (BioRad) and then transferred to nitrocellulose membranes (Schleicher & Schuell). After blocking, the membranes were probed with mouse antibodies diluted 1/1000 in milk. The antibodies used were against: p(Ser473)Akt, Akt, p(Ser536)NFκB p65, p(Ser176/180) IKKα/β p(Ser9)GSK-3β and β-actin (Cell Signaling Technology). Antibody binding was revealed with a peroxydase-coupled secondary antibody diluted in milk, detected using the Amersham ECL Plus reagent (GE Healthcare) and quantified by Image Quant TL software (GE Healthcare Bio-sciences). The membranes were stripped and re-probed with the anti-β-actin antibody as a control for loading. Insulin signaling molecule phosphorylation was performed in stimulated state after an euglycemic hyperinsulinemic clamp procedure.

2.11. RNA extraction and quantification

All tissues were homogenized in TRIzol Reagent (Life Technologies) prior to extraction. RNA integrity was evaluated using an Experion Automated Electrophoresis Station (Biorad). Samples with a RIN over 7.8 were reverse transcribed by using a cDNA Reverse Transcription Kit (Applied Biosystems) according to the manufacturer's protocol. The Fluidigm high-throughput qPCR method (Biomark) was used as described in Protocol n°37 from the manufacturer. Each primer (see Supplementary Information) was tested by LinRegPCR software and amplification efficiency was over 80%. Data were analyzed using the Fluidigm Real-Time PCR Analysis software. qPCR reactions were performed on a ViiA7 Real-Time PCR System (Life Technologies). Data were analyzed with the ViiA7 RUO Real-Time PCR analysis software. Primer sequences are reported in Supplementary Information. Relative RNA quantity was determined by the $2-\Delta Ct$ method using RPL19 as reference transcript.

2.12. 16S rRNA-DNA sequencing analysis

The microbial population in the luminal ileum content and the ileum mucosa (washed its luminal contents) were analyzed by high-throughput sequencing of variable regions of the 16S rRNA bacterial gene (Vaiomer SAS, Labège Innopole, France). Genomic DNA was isolated from ileum samples using a tissue-specific extraction technique optimized for whole ileum samples. The total genomic DNA was prepared in a final volume of 50 μl. DNA concentrations were determined by UV spectroscopy in a Nanodrop®2000 (ThermoScientific). PCR amplification was performed using 16S universal primers targeting the V3-V4 region of the bacterial 16S ribosomal gene (Vaiomer universal 16S primers). The joint pair length of the amplicon encompassed 476 base pairs using 2 × 300 paired-end Miseq kit V3. For each sample, a sequencing library was generated by addition of sequencing adapters. The detection of the sequencing fragments was performed using MiSeq Illumina® technology. The targeted metagenomic sequences from tissue microbiota were analyzed using the bioinformatics pipeline established (www.vaiomer.com). Briefly, after demultiplexing of the bar-coded Illumina-paired reads, single read sequences for each sample were cleaned and paired for each sample independently into longer fragments. After quality filtering and alignment against a 16S reference database, clustering into OTU (Operational Taxonomic Unit) with a 97% identity threshold and taxonomic assignment were performed to determine community profiles.

2.13. Quantification of bacterial 16S rDNA and protein concentration in intestine

Total DNA was extracted from frozen luminal or mucosal ileum contents by using the QIAamp DNA Mini Stool Kit (Qiagen) following the manufacturer's instructions. Prior to extraction, tissues were homogenized with beads of ≤106 μm diameter in a Precellys24 high-throughput tissue homogeniser (Ozyme) for 2 × 30 s at 5500 rpm. The DNA was amplified in a StepOne Real-Time PCR System (Applied Biosystems) in optical-grade 96-well plates (Applied Biosystems). The PCR reaction used a master mix (Power SYBR Green master mix; Life Technologies) as described previously [28]. The concentration of 16S rRNA DNA was normalized to the total DNA concentration.

2.14. Quantification of IgA in cecum content

Cecum contents were collected, immediately frozen at −70 °C and lyophilized. After recording the net dry weight for each sample, extracts were prepared by adding PBS with a protease inhibitor cocktail (Roche) in a ratio of 20 μl per mg dry cecum content, as described [29]. Solid matter was suspended by extensive vortexing followed by centrifugation at 16,000 × *g* for 10 min. Supernatants were stored at −20 °C and IgA concentration was quantified by ELISA using the mouse IgA ELISA Quantitation Set (Bethyl Laboratories) according to the manufacturer's procedure.

2.15. Data analysis

Data handling, analyses and graphical representations were performed using Microsoft Excel and GraphPad Prism. Statistical significance ($p < 0.05$) was determined using a Student's *t* test, one-way or two-way ANOVA and were annotated using the international convention related to the statistical representation. Data with no significant differences were represented with similar superscript letter. Principal component analyses (PCA) were performed using the mixOmics R Package [30].

3. RESULTS

3.1. Immunization with ileum contents protects against HFD-induced glucose intolerance

To study the effect of immunization with gut bacteria on the development of metabolic disease, mice were injected subcutaneously with dilutions of the ileum contents from HFD-fed mice. 35 days later, immunized mice were fed a HFD to challenge their metabolic homeostasis, and we determined whether the immunization procedure prevented the impairment of metabolic parameters induced by the HFD (Figure 1A). After one month of HFD, mice immunized with ileum contents diluted 1/5000 or 1/500 were protected against HFD-induced glucose intolerance when compared to the non-immunized mice (Supplementary Figure S1A,B and Figure 1B,C). This protection lasted during the two months of the experiment, while the mice were fed the HFD (Figure 1F,G). This effect was not observed with the 1/100 dilution of ileum contents (Supplementary Figure S1A,B). The dilution of 1/5000 was chosen for the rest of the study. The immunization did not affect the glycemic parameters of mice fed a NC diet (Supplementary Figure S1C,D), and body weight was unchanged (Supplementary Figure S1E), suggesting a decrease in their food intake. However, due to the soft consistency of the diet, we could not properly record this data set. Furthermore, the fasting hyperglycemia, hyperinsulinemia, glucose intolerance and impaired glucose-induced insulin secretion observed in HFD-fed mice were normalized by the immunization (Figure 1B—H**)**. Immunization also improved HFD-induced insulin resistance (Figure 1I). Consistent with these results, Akt phosphorylation in muscle and liver and GSK3β in muscles, assessed at the end of the clamp procedure, were normalized in the immunized mice to the level seen in NC-fed mice (Figure 1J—M). Liver steatosis, i.e. triglyceride accumulation, was not affected by the immunization during the two month follow up (Supplementary Figure S1F). Altogether, the immunization procedure first affected insulin action and glycemic control, which then sequentially controlled body weight and other metabolic parameters. Interestingly, the immunization procedure with ileum contents from NC-fed mice also improved the glucose tolerance of HFD-fed mice (Supplementary Figure S2A—C), but this effect was transient and lasted only for one month **(**Supplementary Figure S2A—E). Moreover, mice immunized with the luminal ileum contents from germ-free mice (Supplementary Figure S2F,G) or from antibiotic-treated HFD-fed mice were not protected against HFD-induced glucose intolerance (Supplementary Figure S2H,I), suggesting that the antigens responsible for protection against HFD-induced diabetes are most likely of microbial origin.

Therefore, to gain knowledge about the components associated with the immunization efficacy, we quantified whether the luminal gut microbiota was altered by HFD. We performed 16S rRNA-DNA-based quantification and characterization on the contents of the ileum. We focused our attention on this intestinal segment since recent data from our laboratory demonstrated its importance on the control of metabolic disease and bacterial translocation [5,22]. Although the concentration of bacterial rRNA-DNA was similar in NC- and HFD-fed mouse luminal ileum content (Supplementary Figure S3A), the number of colony forming units (cfu) of aerobic bacteria was reduced in the luminal ileum content from HFD-fed mice when compared to those from NC-fed mice (Supplementary Figure S3B,C). To qualify these differences, we performed 16S rRNA-DNA targeted metagenomic sequencing. The 16S rRNA-DNA sequences differed between the HFD-fed and NC-fed mice (Supplementary Figure S3D,E). In contrast to what was observed in feces, the bacterial community was more diverse in the luminal ileum content of HFD-fed mice than in NC-fed mice. The proportion of *Porphyromonadacaea* decreased in response to HFD, whereas the frequencies of *Burkholderiaceae*, *Sphingomonadaceae*, *Peptostreptococcaceae*, *Phyllobacteriaceae*, and *Sutterellaceae* increased (Supplementary Figure S3E). Moreover, the protein concentration of the luminal ileum content from HFD-fed mice was lower than that of control mice (Supplementary Figure S3F), and the quality of the proteins between groups differed as evaluated from trypsin-digested proteins by using nanoHPLC-Chip followed by MS/MS technology (Supplementary Figure S3G,H and Supplementary Table S1). Altogether, these analyses show that the luminal ileum content differs between HFD and NC-fed mice in term of bacterial taxa. These differences could be responsible for the efficacy of the immunization procedure protecting against HFD-induced hyperglycemia. The mechanism responsible for the immunization procedure, therefore, remains to be identified.

3.2. Impact of immunization with ileum contents on liver and muscle metabolic inflammation

Metabolic disease is characterized by a low grade inflammation, which precedes the development of insulin resistance and hyperglycemia [31,32]. To investigate whether immunization with the luminal ileum content from HFD-fed mice affects metabolic inflammation, we quantified the cytokine mRNA concentrations and signaling phosphorylated proteins in muscle and liver after one month of HFD (i.e. 65 days post immunization). In muscle, the immunization procedure decreased the mRNA concentrations of inflammatory cytokines CCL2, IL1β and PAI1 (Figure 2A). Conversely, the anti-inflammatory cytokine IL4 increased in immunized mice (Figure 2A), suggesting that metabolic inflammation was toned down by the immunization process. However, the relative levels of the phosphorylated forms of main downstream effectors of inflammation, such as NF-κB and IKKβ, were unaffected by diet or immunization (Figure 2C—E), suggesting that a change in metabolic inflammation, despite the increased cytokine mRNA concentration, was not triggered by the immunization process. This was confirmed in the liver since no major differences in inflammatory or anti-inflammatory mRNA concentrations were observed (Figure 2B). Although, phosphorylation of NF-κB was not statistically affected by diet or immunization, an increase in IKKβ phosphorylation was observed in HFD-fed mice, and this was normalized by the immunization process (Figure 2C,F,G). In the absence of a clear role played by the inflammatory process, cytokines and related inflammatory markers, we quantified the leukocyte numbers from the liver of immunized and non-immunized mice (Figure 2H). T lymphocytes (Figure 2I) and antigen presenting cells (APC) (Figure 2J) were quantified by flow cytometry. No differences in the total numbers of liver leukocytes or T lymphocytes and APCs were observed between immunized and non-immunized HFD-fed mice (Figure 2H—J). In mesenteric AT, except for CD11c and Foxp3 mRNA levels, which decreased in immunized mice, no statistically significant differences in inflammatory markers were observed (Supplementary Figure S4). Altogether, these results show a minor improvement of inflammation in liver and VL muscle in immunized mice, indicating that this is not the major mechanism triggered by

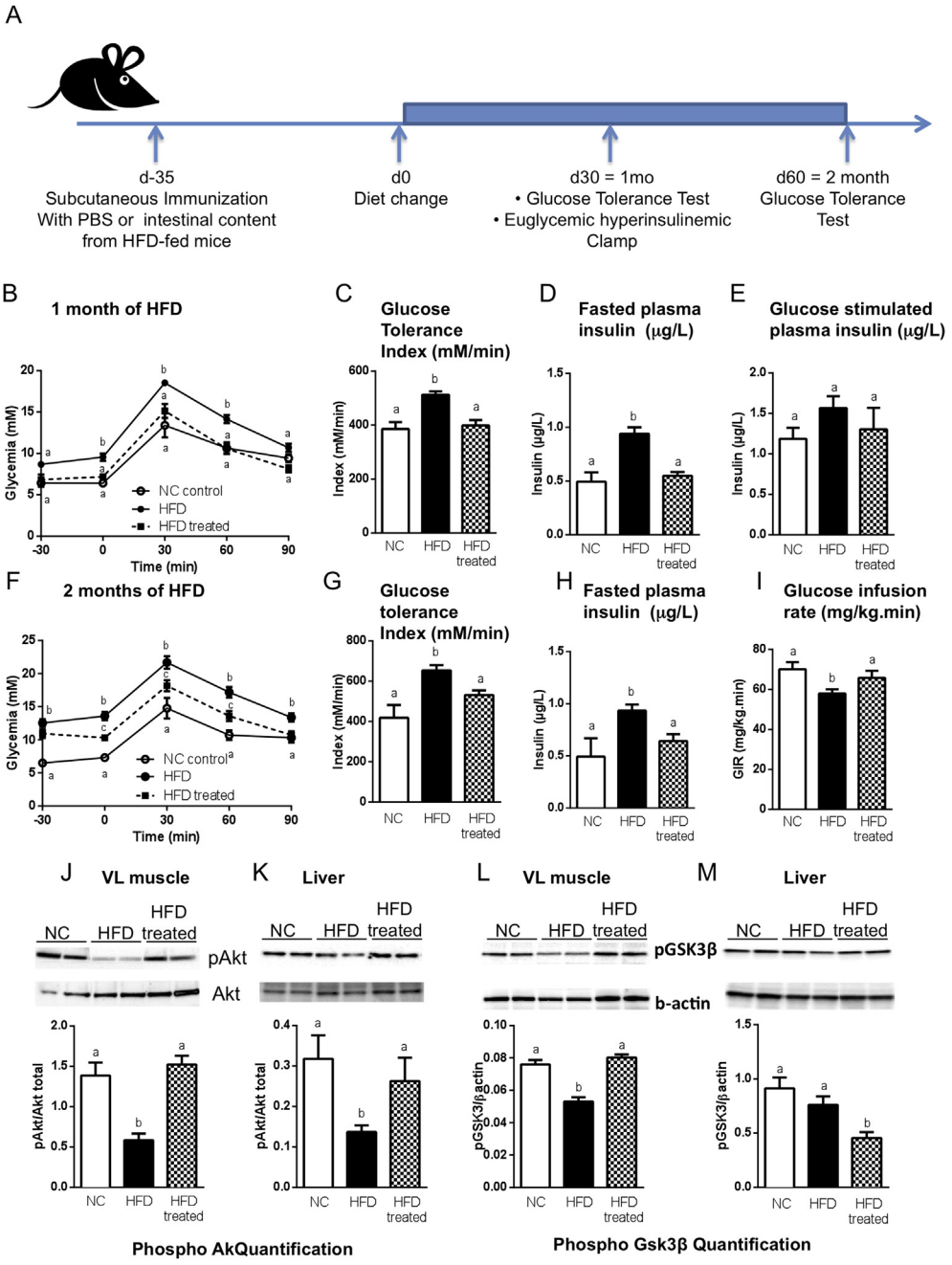

Figure 1: Immunization with the contents of the ileum protects against HFD-induced insulin resistance and dysglycemia. C57Bl/6 mice were immunized s.c. with 200 µl of either PBS (●,o) or the ileum contents from mice fed a high-fat diet (treated; ■). Thirty-five days later, mice were fed either normal chow (NC) or a high-fat diet (HFD) as illustrated in (A). (B–E) After one month of HFD, an intraperitoneal glucose tolerance test (ipGTT) (B) was performed and the metabolic index (C) was calculated. Fasting (D) and glucose-stimulated (E) plasma insulin concentrations were quantified (µg/l). (F–H) After two months of HFD, ipGTT (F) was performed, the metabolic index (G) was calculated and the fasting (H) plasma insulin concentration was calculated. (I) Glucose infusion rate was calculated (mg $\times$ kg^{-1} $\times$ min^{-1}) by means of steady-state euglycemic (5.5 mmol/l) hyperinsulinemic clamping (18 mU $\times$ kg^{-1} $\times$ min^{-1}) of mice after one month of HFD. (B–I) Data are means $\pm$ SEM. n = 6 mice/group; data show one experiment out of three. Data with similar superscript letters (a,b) indicate data non-statistically different between each other at a probability threshold $p > 0.05$. (J–M) Quantification of phosphorylated Akt (J,K) and phosphorylated GSK3β (L,M) in the muscle (VL) (J,L) and in the liver (K,M) after euglycemic hyperinsulinemic clamp procedure. The arbitrary units indicate the ratio of phosphorylated protein to β actin. Data are means $\pm$ SEM. n = 3–4 mice/group. Data with similar superscript letters (a,b) indicate data non-statistically different between each other at a probability threshold $p > 0.05$.

the immunization procedure. A role of the intestinal immune system could be suggested since we previously showed that during HFD-induced type 2 diabetes an early reduction in the number of Th17 cells was causally responsible for the glycemic control [5].

3.3. Immunization with ileum contents targets the adaptive immune response

The ileum microbiota dysbiosis induced by HFD treatment and its efficacy in the control of glycemia and insulin action in response to the

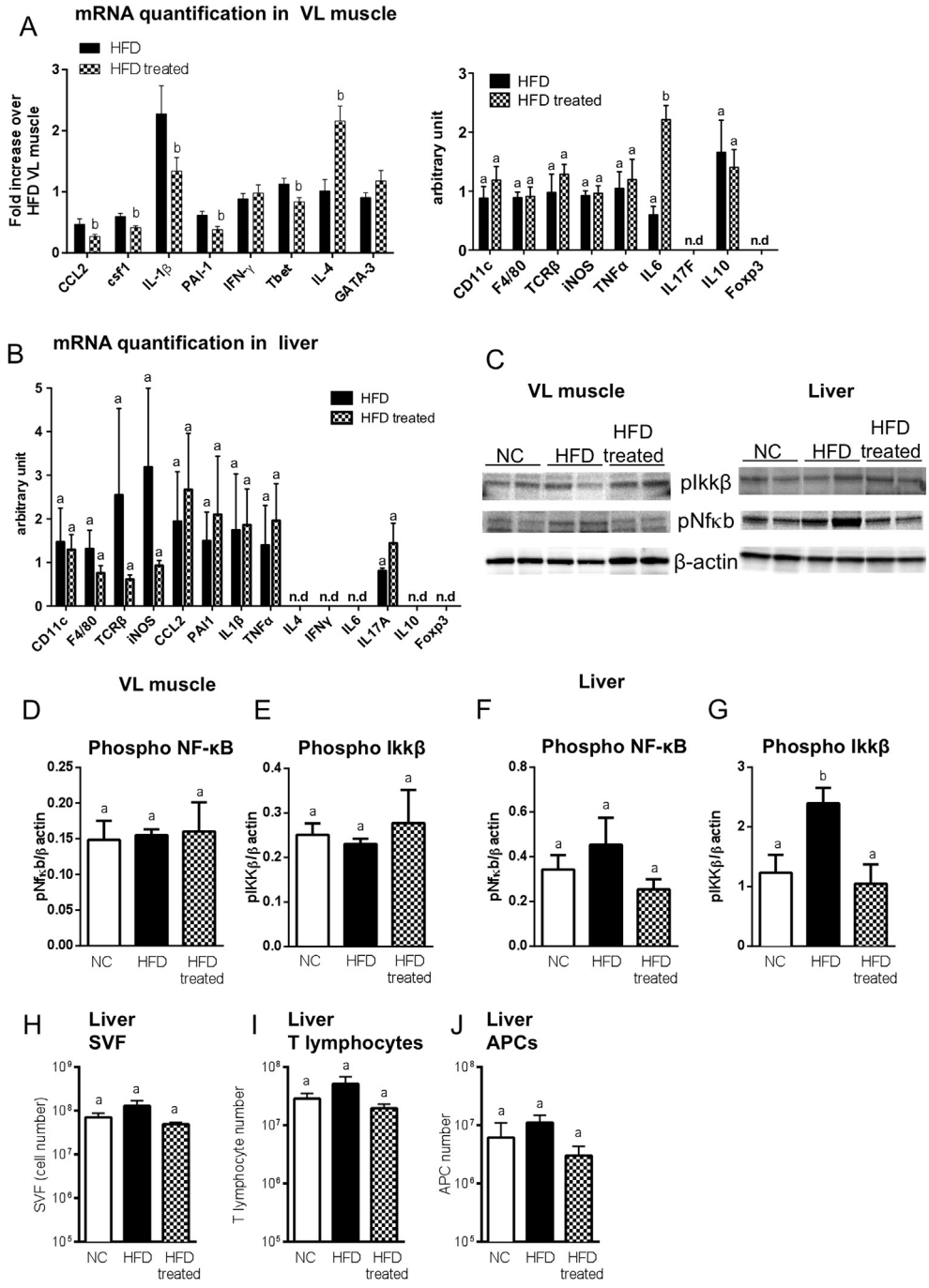

Figure 2: Immunization with the contents of the ileum decreases tissue inflammation. C57Bl/6 mice were injected s.c. either with 200 μl of PBS or with the ileum contents from mice fed a HFD (treated). 35 days later, mice were fed a HFD or NC. After one month of HFD, immune markers including proinflammatory and anti-inflammatory cytokine mRNAs were quantified from VL muscle (A) and liver (B) from non-immunized (HFD) or immunized (HFD treated) mice fed a HFD. Data are means ± SEM; n = 5–6 mice/group. Data with similar superscript letters (a,b) indicate data non-statistically different between each other at a probability threshold $p > 0.05$. (C) Western blotting of phosphorylated proteins in VL muscle (left) and in liver (right) after one month of HFD. Phosphorylation of NF-κB and IKKβ was quantified in the muscle (D,E) and in the liver (F,G). Data are means ± SEM. n = 3–4 mice/group. Data with similar superscript letters (a,b) indicate data non-statistically different between each other at a probability threshold $p > 0.05$. (H–J) Leukocytes were isolated from livers of NC mice (n = 5; NC), HFD-fed non-immunized mice (n = 8; HFD) and HFD-fed immunized mice (n = 7; HFD treated). Cell numbers were determined in (H). (I) T lymphocytes (CD45 + TCRβ+) and (J) APCs (CD45 + CD19-MHCII+) number were determined by flow cytometry. Data are means ± SEM. Data with similar superscript letters (a,b) indicate data non-statistically different between each other at a probability threshold $p > 0.05$.

immunization procedure led us to suggest that the adaptive immune system is likely to be involved. Therefore, we first evaluated CD4 and CD8 T cell responses in the draining lymph nodes (LN) and in the spleens of NC-fed mice ten days after immunization during the acute phase of activation of T cells and before the induction of glucose intolerance. CD4 and CD8 T cells from the immunized mice proliferated more than those from non-immunized mice in the LN (Figure 3A,B) as opposed to what observed from the spleen (Supplementary

Figure S5A,B). The proportion of IFNγ- or TNFα-producing CD4 and CD8 T cells from the draining LN and spleen was also higher in immunized mice compared to non-immunized mice (Figure 3C,D and Supplementary Figure S5C,D), further demonstrating the involvement of the adaptive immune system in response to the microbiota treatment on the control of metabolic phenotypes. By contrast, the proportions of IL17-producing CD4 T cells were not affected by the immunization (Figure 3C and Supplementary Figure S5C). IL4-producing CD4 T cells were not detectable (data not shown) and Foxp3+ regulatory cells were not affected in the LN while they were decreased in spleen (Figure 3E and Supplementary Figure S5E), ruling out a role of these immune cells. Overall, these data show that immunization with ileum microbiota from HFD-fed mice induces acute systemic CD4 and CD8 T cell responses.

To determine whether this immunization was long lasting and able to generate memory T cells, we characterized CD4 and CD8 T cell responses 35 days after immunization. The proportions of IFNγ- and TNFα-producing CD4 and CD8 T cells remained higher in the LN and in the spleen in the immunized mice compared to non-immunized mice (Figure 3F,G and Supplementary Figure S5F,G). The proportions of IL17-producing CD4 T cells remained unchanged in this memory phase (Supplementary Figure S5F). It is noteworthy that CD4 and CD8 T cells from draining LN and the spleen were characterized by similar cytokine secretion profiles (Figure 3F,G and Supplementary Figure S5F,G), suggesting that they were in a similar activation state. In addition, 35 days post-immunization, the plasma concentrations of IgG1, IgG2a and IgG2b were increased in the immunized mice as compared to the control mice, implying a role for B cells (Figure 3H). Overall, these results show that immunization induced a memory immune response that could be responsible for the protection against HFD-induced hyperglycemia.

3.4. Passive immunization protects against HFD-induced glucose intolerance and requires adaptive immunity

To demonstrate that immunization with luminal ileum contents induces a protective memory immune response, we transferred immune cells

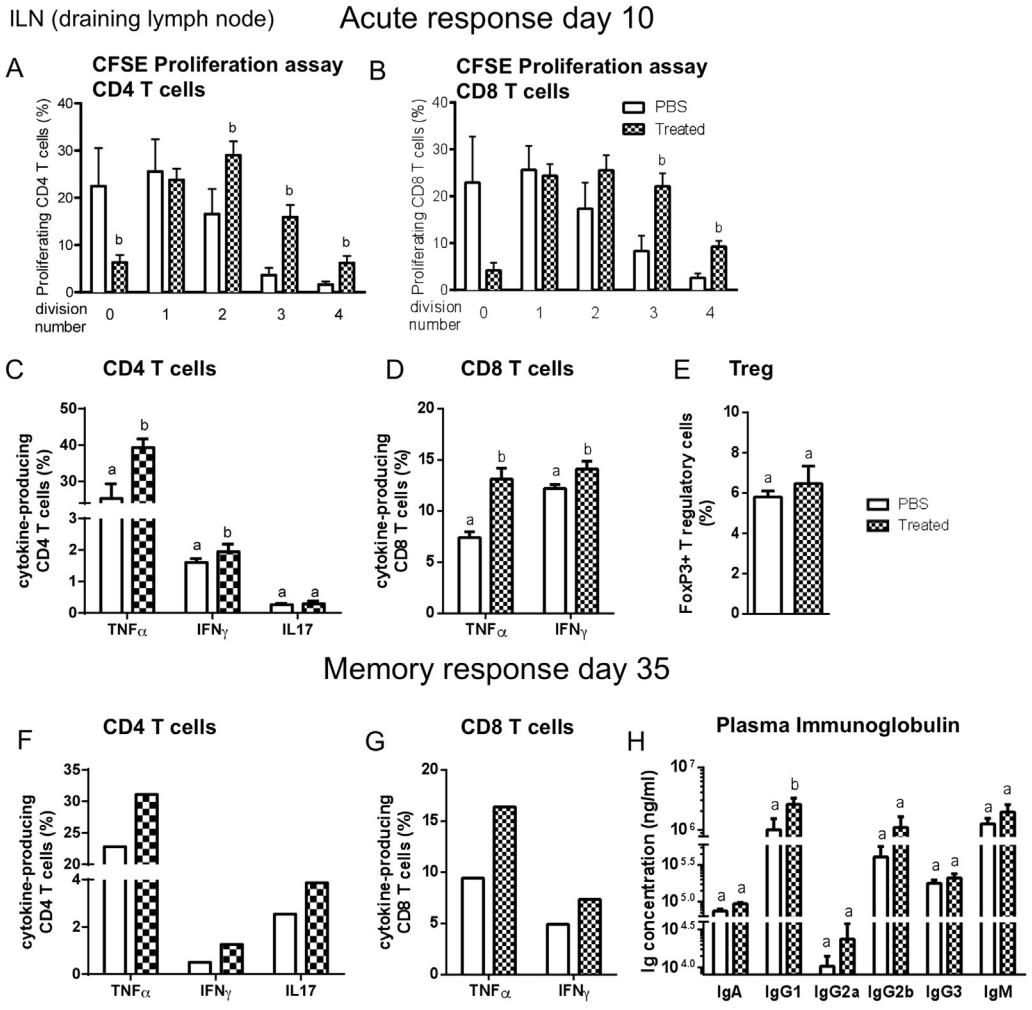

Figure 3: Immunization with the contents of the ileum increases T cell responses. Mice were injected s.c. with PBS or with the ileum contents from mice fed a HFD (treated). (A—E) 10 days later, draining (inguinal) LN cells were labeled with CFSE to assess T cell proliferation during stimulation with plate-bound anti-CD3/CD28 for 3 days. The percentage of CD4 (A) or CD8 (B) T cells in the population was determined at each round of division. (C—E) The functionality of T cells was measured by *ex vivo* stimulation of LN cells. The percentage of CD4 (C) and CD8 (D) T cells producing IFNγ, TNFα, IL17 in response to stimulation was determined. (E) The percentage of Foxp3+ Tregs among total lymphocytes in draining LNs. (A—E) Data are means ± SEM; n = 6 mice per group. (F—G) 35 days after immunization, the proportions of CD4 (F) and CD8 (G) T cells producing cytokines (IFNγ, TNFα, IL17) were quantified following *ex vivo* stimulation of inguinal LN cells from mice injected with PBS or ileum contents (Treated) (n = 8 mice pooled per group, one experiment representative of two). (H) Concentrations of IgA, IgG and IgM (ng/ml) in the plasma from mice injected with PBS or ileum contents as in parts (F) and (G). Data are means ± SEM; n = 6 mice per group. Data with similar superscript letters (a,b) indicate data non-statistically different between each other at a probability threshold $p > 0.05$.

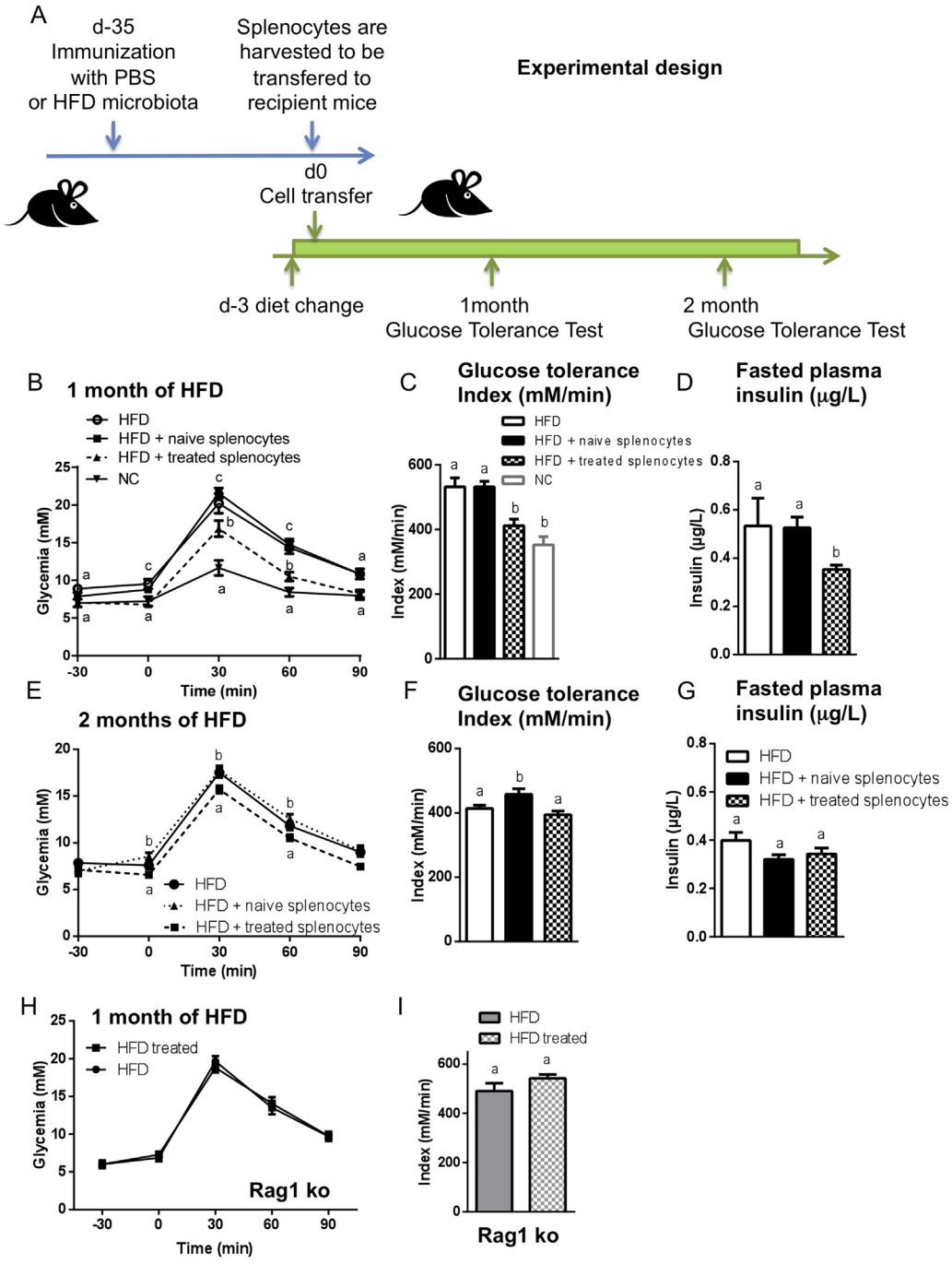

Figure 4: Adoptive transfer of immune cells protects against HFD-induced insulin resistance and dysglycemia. (A–G) 3×10^7 splenocytes from CD45.1 mice injected with PBS (■; naive splenocytes) or with the ileum contents from mice fed HFD (▲; treated splenocytes) were transferred into CD45.2 naïve recipients fed HFD, as summarized in (A). (B,E) Intraperitoneal GTTs were performed after one month (B) and two months (E) of HFD. Glucose tolerance indices were calculated (C,F). (D,G) Fasting plasma insulin was quantified (µg/ml). Data are means ± SEM; n = 8 mice per group. Data with similar superscript letters (a,b) indicate data non-statistically different between each other at a probability threshold $p > 0.05$. (H,I) Rag1-deficient mice (Rag1 ko) were injected s.c. with 200 µl of PBS (●) or with the ileum contents from mice fed the HFD (HFD treated; ■). Thirty-five days later, the mice were fed HFD. After one month of HFD, an intraperitoneal GTT (H) was performed and the glucose tolerance index (I) was calculated. Data are means ± SEM. n = 5 mice/group. Data with similar superscript letters (a,b) indicate data non-statistically different between each other at a probability threshold $p > 0.05$. The experiment was performed twice.

harvested either from spleen or from draining LN of immunized CD45.1 mice 35 days post immunization into recipient naïve CD45.2 mice that were fed a HFD for three days before cell transfer (Figure 4A). After one month of HFD, the recipient mice were protected from HFD-induced impairments (Figure 4B–D) for roughly two months (Figure 4E–G). The transferred cells were detected in the spleen and the LN for two months after adoptive transfer (Supplementary Figure S6A–H). The protection was not observed in mice lacking lymphocytes (Rag1-deficient

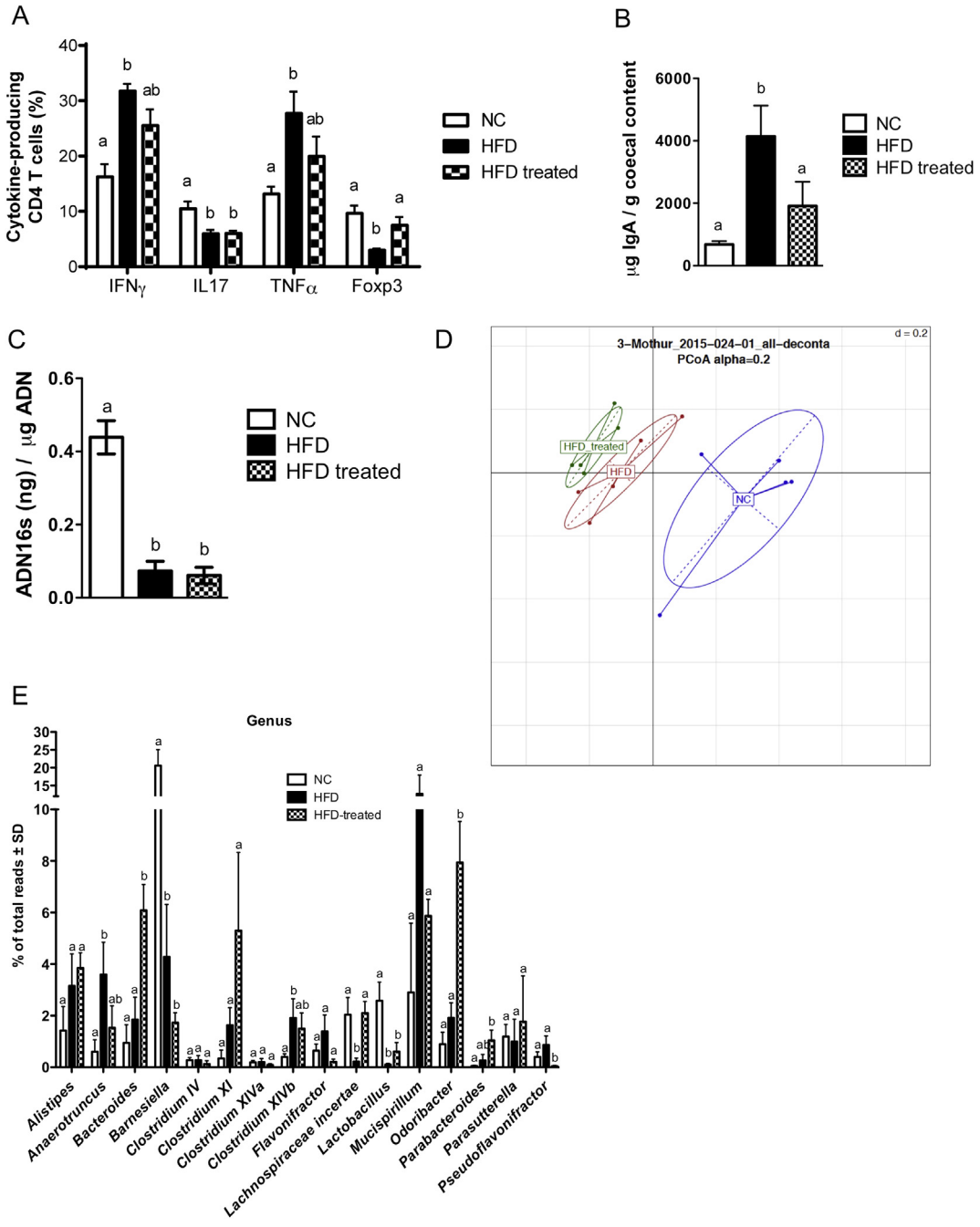

Figure 5: Immunization with ileum content modifies intestinal immunity and ileum microbiota. C57Bl/6 mice were immunized s.c. with 200 µl of either PBS or the ileum contents of mice fed HFD (treated). Thirty-five days later, mice were fed either NC or HFD as illustrated in (Figure 1A). (A) After one month of HFD, SILP leukocytes (CD4 + TCRβ + CD45+ cells) from mice fed NC, HFD or HFD treated mice were analyzed by flow cytometry. Proportion of IFNγ, TNFα and IL17-producing CD4 T cells upon stimulation and Foxp3 CD4 T cells. Graphs show mean ± SEM; n = 5 mice per group, one experiment representative of two. Data with similar superscript letters (a,b) indicate data non-statistically different between each other at a probability threshold $p > 0.05$. (B) After one month of HFD, IgA concentration was measured in cecum contents from mice fed NC, HFD or from HFD treated mice, by ELISA. Graphs show mean ± SEM; n = 5 mice per group. Data with similar superscript letters (a,b) indicate data non-statistically different between each other at a probability threshold $p > 0.05$. (C–E) Quantification and characterization of the microbial composition of ileum mucosa of NC, HFD and HFD treated mice. (C) 16S rDNA concentration. (D) 16S rRNA-DNA gene sequencing analysis of the ileum mucosa microbiota. Principal Coordinate Analysis (PCoA); (E) Frequency of major bacterial genera in NC, HFD or HFD treated mice obtained from ileum mucosa 16s rRNA-DNA gene sequencing analysis. Graphs show mean ± SEM; n = 5 mice/group; Data with similar superscript letters (a,b) indicate data non-statistically different between each other at a probability threshold $p > 0.05$.

mice) (Figure 4H,I). Overall, these results demonstrate the central role of adaptive immunity in the protection induced by the immunization procedure. The remaining question is the mode of action by which the central role of the adaptive immunity protects against hyperglycemia.

3.5. Immunization with ileum content modifies intestinal immunity and ileum microbiota

We and others have demonstrated a causal role of intestinal adaptive immunity, more precisely intestinal CD4 T cells, in HFD-induced insulin

resistance [5,33]. Therefore, we monitored CD4 T cell subsets in the ileum of HFD-fed mice previously immunized or not with ileum contents, after one month of HFD (i.e. 65 days post immunization). As expected [5], HFD increased the frequency of IFNγ-producing CD4 T intestinal cells while reducing the frequency of Foxp3-expressing and IL17-producing CD4 T cells in the *lamina propria* when compared to NC-fed mice (Figure 5A). We also observed an increase of the proportion of TNFα-producing CD4 T cells in HFD-fed mice. Immunization prevented the loss of Foxp3-expressing cells and modestly increased the frequency of IFNγ- and TNFα-producing CD4 T cells while not affecting the decreased proportion of IL17-producing CD4 T cells, showing that microbiota-based immunization selectively involves the adaptive immune system for the control of metabolic features. We also observed an increased IgA concentration in the cecum content of mice fed a HFD for 35 days, which was reversed by the immunization procedure (Figure 5B).

Since HFD-induced gut microbiota dysbiosis is causally involved in metabolic disease [5], immunization could control this mucosal feature. We have previously demonstrated that HFD changed the microbial composition of the ileum mucosa [5]. To evaluate whether the gut microbiota was controlled by the immunization procedure, we performed 16S rRNA-DNA-based quantification and characterization of the ileum mucosa. First, we observed a similar decrease in the concentration of bacterial rRNA-DNA in the ileum mucosa of HFD and HFD treated mice (Figure 5C). However, the 16S rRNA-DNA gene sequencing of the ileum mucosa and the principal coordinate analysis revealed changes in the microbial composition of the ileum mucosa from HFD mice previously immunized with luminal ileum contents, compared to non-immunized HFD mice (Figure 5D). The relative abundance of *Bacteroides, Odoribacter, Parabacteroides* and *Pseudoflavonifractor* was impacted by the immunization procedure. Furthermore, the immunization also reversed some bacterial genera modified by the HFD, such as *Anaerotruncus*, *Lachnospiraceae incertae* and *Mucispirillum* (Figure 5E). However, mRNA concentrations for epithelial tight junction proteins and anti-microbial peptides were not impacted by the immunization (Supplementary Figure S7), while the plasma LPS concentration was reduced in HFD-fed mice that were previously immunized (Supplementary Figure S8). Overall, we showed that immunization with luminal ileum contents prior to HFD feeding improved insulin action, targeted precise microbial genera and reversed HFD-induced changes in the intestinal CD4 T cell response.

4. DISCUSSION

We show here that immunizing mice with the luminal intestinal contents from the ileum of HFD-fed mice induces an adaptive immune response involving both T and B lymphocytes that controls the onset of HFD-induced insulin resistance and dysglycemia. This occurs as a result of the immunization acting on the adaptive immune system, which impacts intestinal immunity and prevents the deleterious effect of HFD on gut microbiota dysbiosis. Altogether, our findings demonstrate that metabolic diseases are regulated by the relationship between the small intestine mucosal microbiota and the corresponding intestinal adaptive immune system.

We here focused on the role played by the ileum microbiota from HFD-fed mice since we had previously shown that bacterial adhesion and translocation to the ileum mucosa was increased during HFD-induced metabolic disease [5,22]. The causal role of the ileum microbiota from HFD-fed mice in metabolic disease was demonstrated in germ free mice colonized with the corresponding microbiota [5]. Although we cannot rule out a role of the microbiota from other intestinal segments, we hypothesized that during the course of HFD-induced metabolic disease, inappropriate immune responses develop which could be modified by immunization with ileum microbiota. The change in ileum microbiota in HFD-fed mice could be linked to the fat content itself, which is very high. For example, this very high-fat diet could trigger the production of more bile acids than would normal chow. The primary bile acids produced by the liver and released into the duodenum are substrates of the microbiota leading to secondary bile acids, which then could have a role on the immune system. We previously showed that drastic changes in the intestinal immune system occur in the ileum, rather than in the colon, in response to a fat-enriched diet [5]. Furthermore, germ free mouse colonization demonstrated that the dysbiotic microbiota from the ileum of diabetic mice was causal to immune changes in this intestinal segment [5]. Altogether, these observations strongly suggest that the interaction between the ileum microbiota and the ileum immune system represents an important dyad for the control of glycemia. To test this hypothesis, we challenged the immune system by injection of luminal ileum microbiota and demonstrated the impact of HFD on the induction of insulin resistance. The antigens and triggering factors involved are unknown but certainly recruit lymphocytes. As shown here, the improvement of metabolic parameters, such as insulin resistance and glucose tolerance, following immunization might be due to the re-education of the immune system against the 'diabetic dysbiotic' microbiota in lymphoid organs. Interestingly, some degree of protection against HFD-induced insulin resistance was also observed when mice were immunized with the luminal ileum contents of NC-fed mice. Although we show here that the luminal ileum microbiota differs between NC- and HFD-fed mice, some bacterial genera were common between the groups suggesting that common components may have contributed to this protective effect. However, the protection was shorter suggesting that the common components were insufficient to maintain protection after this first month. Furthermore, although the immunization process using the luminal ileum content was not from germ free mice fed a fat-enriched diet we do rule out a role for fat components since the immunization with the intestinal content from antibiotic-treated HFD-fed mice did not provide any efficient protection.

Differences in the concentration of microbiota used to immunize can clearly affect the level of protection since immunization with a high dose of microbiota (1/100) was less protective than a low dose (1/5000). Detrimental effects of high antigen doses on the adaptive immune response have been reported previously, for example, due to T cell exhaustion in an acute infection model [34]. Moreover, the dose of antigen can affect which subsets of CD4 T cells are induced: a high dose of antigen is reported to induce preferentially T follicular helper cells [35]. The adaptive immunity induced by a high dose of antigen, therefore, might differ from that induced with a low dose. Hence, the immune response induced by high dose might not be protective against insulin resistance.

It is well accepted that gut microbiota is tolerated by the intestinal immunity [36]. However, this tolerance might be restricted to the intestine and possibly rose when gut antigens are presented differentially to immune cells, such as following immunization. Indeed, we report here that 10 days following immunization, the proliferation and cytokine production of CD4 and CD8 T cells are increased in draining LN of immunized mice compared with non-immunized mice. It is noteworthy that the activation of CD4 and CD8 T cells in LN observed at day 10 post immunization does not preclude a further change in muscle inflammation when the mice are challenged by the HFD treatment i.e. 65 days post immunization. The activation of the CD4 and CD8 T cells by the immunization process is transient and followed by the development of

immune memory. Therefore, it is not expected that the muscle would undergo an inflammatory process mediated by the CD4 and CD8 T cells from the corresponding LN. The mechanism responsible for improved insulin sensitivity seems to be linked to factors other than a change in liver and muscle metabolic inflammation. Therefore, we studied the impact of the immune system on the prevention of the deleterious impact of gut microbiota dysbiosis induced by a HFD. We observed that the immunization prevents the changes in the intestinal CD4 T cell population induced by HFD. Our data confirm those of others showing that IFNγ-producing CD4 T cells are increased in response to HFD [33]. Furthermore, we also show that the immunization process impacts precise bacteria of the ileum mucosal microbiota. This is in line with others [37], who have shown that the intestinal immunity can shape the gut microbiota and influence inflammatory bowel disease. We cannot rule out that the immunization procedure could have inhibited food intake and therefore, could be responsible for the improved glycemic phenotype reported here. In addition, as a consequence of a change in food intake one could suggest that the secretion of bile acids would be different which could hamper the gut microbiota ecology do to their detergent effect. This hypothesis remains to be tested. Altogether, we show that targeting the adaptive immune system by specific luminal ileum microbiota extracts allows the intestinal immune system to control gut microbiota most likely through the activation of CD4 T cells and the production of IgA. This mechanism is largely documented where a change in gut microbiota, by the mean of antibiotics or prebiotics and by germ free mouse colonization, is responsible for the glycemic control. We, therefore propose that the immunization process impacts the glycemic control by a mechanism involving the adaptive intestinal immune system.

5. CONCLUSION

Our demonstration that, first, immunization with the luminal ileum microbiota from HFD-fed mice can improve glycemic control suggests new avenues for the treatment and prevention of T2D by vaccination. Second, the clear impact of our immunization approach on the adaptive immune system and gut microbiota dysbiosis provides further evidence of the causal role of the crosstalk between the gut microbiota and the immune system on the control of metabolism. This concept could be extended to other inflammatory diseases, such as atherosclerosis, in which the microbiota plays a triggering role [38].

ACKNOWLEDGMENTS

We would like to thank Drs. Victorine Douin, Nicolas Fazilleau, Christophe Heymes, Chantal Chabo and Xavier Collet for helpful discussions and Dr. Fredrik Bäckhed for preparing the germ-free mouse intestinal contents. We thank J-J. Maoret and F. Martins from the Quantitative Transcriptomic Facility (I2MC Inserm/UPS UMR1048) and A. Zakaroff and C. Pecher from the Flow Cytometry Facility (I2MC Inserm/UPS UMR1048), Y. Barreira and her team from the Animal Care Facility of Rangueil Hospital (UMS US006/Inserm), and S. Le Gonidec and A. Desquesnes from the Phenotyping Facility (UMS US006/Inserm) for their technical support. This work was supported by grants from the Agence Nationale de la Recherche (Bactimmunodia (BSV1 02301), Transflora (08-BLAN-0324), Floradip (GENOPAT 2009)) to RB, from the European Association for the Study of Diabetes, MSD, to LG, from the Région Midi-Pyrénées to RB and from the Société Francophone de Diabétologie to CP.

APPENDIX A. SUPPLEMENTARY DATA

Supplementary data related to this article can be found at http://dx.doi.org/10.1016/j.molmet.2016.03.004.

CONFLICT OF INTEREST

RB owns shares in vaiomer.

REFERENCES

[1] Qin, J., Li, Y., Cai, Z., Li, S., Zhu, J., Zhang, F., et al., 2012. A metagenome-wide association study of gut microbiota in type 2 diabetes. Nature 490:55–60.
[2] Ley, R.E., Turnbaugh, P.J., Klein, S., Gordon, J.I., 2006. Human gut microbes associated with obesity. Nature 444:1022–1023.
[3] Velagapudi, V.R., Hezaveh, R., Reigstad, C.S., Gopalacharyulu, P., Yetukuri, L., Islam, S., et al., 2010. The gut microbiota modulates host energy and lipid metabolism in mice. Journal of Lipid Research 51:1101–1112.
[4] Turnbaugh, P.J., Ley, R.E., Mahowald, M.A., Magrini, V., Mardis, E.R., Gordon, J.I., 2006. An obesity-associated gut microbiome with increased capacity for energy harvest. Nature 444:1027–1031.
[5] Garidou, L., Pomie, C., Klopp, P., Waget, A., Charpentier, J., Aloulou, M., et al., 2015. The gut microbiota regulates intestinal CD4 T cells expressing RORgammat and controls metabolic disease. Cell Metabolism 22:100–112.
[6] Dumas, M.E., Barton, R.H., Toye, A., Cloarec, O., Blancher, C., Rothwell, A., et al., 2006. Metabolic profiling reveals a contribution of gut microbiota to fatty liver phenotype in insulin-resistant mice. Proceedings of the National Academy of Sciences U S A 103:12511–12516.
[7] Karlsson, F.H., Fak, F., Nookaew, I., Tremaroli, V., Fagerberg, B., Petranovic, D., et al., 2012. Symptomatic atherosclerosis is associated with an altered gut metagenome. Nature Communication 3:1245.
[8] Tremaroli, V., Karlsson, F., Werling, M., Stahlman, M., Kovatcheva-Datchary, P., Olbers, T., et al., 2015. Roux-en-Y gastric bypass and vertical banded gastroplasty induce long-term changes on the human gut microbiome contributing to fat mass regulation. Cell Metabolism 22:228–238.
[9] Caesar, R., Tremaroli, V., Kovatcheva-Datchary, P., Cani, P.D., Backhed, F., 2015. Crosstalk between gut microbiota and dietary lipids aggravates WAT inflammation through TLR signaling. Cell Metabolism.
[10] Hooper, L.V., Gordon, J.I., 2001. Commensal host-bacterial relationships in the gut. Science 292:1115–1118.
[11] Sommer, F., Backhed, F., 2013. The gut microbiota — masters of host development and physiology. Nature Reviews and Microbiology.
[12] Gaboriau-Routhiau, V., Rakotobe, S., Lecuyer, E., Mulder, I., Lan, A., Bridonneau, C., et al., 2009. The key role of segmented filamentous bacteria in the coordinated maturation of gut helper T cell responses. Immunity 31:677–689.
[13] Ivanov II, , Atarashi, K., Manel, N., Brodie, E.L., Shima, T., Karaoz, U., et al., 2009. Induction of intestinal Th17 cells by segmented filamentous bacteria. Cell 139:485–498.
[14] Atarashi, K., Tanoue, T., Shima, T., Imaoka, A., Kuwahara, T., Momose, Y., et al., 2011. Induction of colonic regulatory T cells by indigenous Clostridium species. Science 331:337–341.
[15] Round, J.L., Mazmanian, S.K., 2010. Inducible Foxp3+ regulatory T-cell development by a commensal bacterium of the intestinal microbiota. Proceedings of the National Academy of Sciences U S A 107:12204–12209.
[16] Mowat, A.M., Agace, W.W., 2014. Regional specialization within the intestinal immune system. Nature Reviews and Immunology 14:667–685.
[17] Suzuki, K., Ha, S.A., Tsuji, M., Fagarasan, S., 2007. Intestinal IgA synthesis: a primitive form of adaptive immunity that regulates microbial communities in the gut. Seminars in Immunology 19:127–135.
[18] Wichner, K., Fischer, A., Winter, S., Tetzlaff, S., Heimesaat, M.M., Bereswill, S., et al., 2013. Transition from an autoimmune-prone state to fatal autoimmune disease in CCR7 and RORgammat double-deficient mice is dependent on gut microbiota. Journal of Autoimmunity 47:58–72.

[19] Medina-Contreras, O., Geem, D., Laur, O., Williams, I.R., Lira, S.A., Nusrat, A., et al., 2011. CX3CR1 regulates intestinal macrophage homeostasis, bacterial translocation, and colitogenic Th17 responses in mice. Journal of Clinical Investigation 121:4787—4795.

[20] Caricilli, A.M., Picardi, P.K., de Abreu, L.L., Ueno, M., Prada, P.O., Ropelle, E.R., et al., 2011. Gut microbiota is a key modulator of insulin resistance in TLR 2 knockout mice. PLoS Biology 9:e1001212.

[21] Albenberg, L., Esipova, T.V., Judge, C.P., Bittinger, K., Chen, J., Laughlin, A., et al., 2014. Correlation between intraluminal oxygen gradient and radial partitioning of intestinal microbiota. Gastroenterology 147:1055—1063 e8.

[22] Amar, J., Chabo, C., Waget, A., Klopp, P., Vachoux, C., Bermudez-Humaran, L.G., et al., 2011. Intestinal mucosal adherence and translocation of commensal bacteria at the early onset of type 2 diabetes: molecular mechanisms and probiotic treatment. EMBO Molecular Medicine 3:559—572.

[23] Burcelin, R., Crivelli, V., Dacosta, A., Roy-Tirelli, A., Thorens, B., 2002. Heterogeneous metabolic adaptation of C57BL/6J mice to high-fat diet. American Journal of Physiology, Endocrinology and Metabolism 282:E834—E842.

[24] Cani, P.D., Bibiloni, R., Knauf, C., Waget, A., Neyrinck, A.M., Delzenne, N.M., et al., 2008. Changes in gut microbiota control metabolic endotoxemia-induced inflammation in high-fat diet-induced obesity and diabetes in mice. Diabetes 57:1470—1481.

[25] Burcelin, R., Uldry, M., Foretz, M., Perrin, C., Dacosta, A., Nenniger-Tosato, M., et al., 2004. Impaired glucose homeostasis in mice lacking the alpha1b-adrenergic receptor subtype. Journal of Biological Chemistry 279:1108—1115.

[26] Garidou, L., Heydari, S., Truong, P., Brooks, D.G., McGavern, D.B., 2009. Therapeutic memory T cells require costimulation for effective clearance of a persistent viral infection. Journal of Virology 83:8905—8915.

[27] Garidou, L., Heydari, S., Gossa, S., McGavern, D.B., 2012. Therapeutic blockade of transforming growth factor beta fails to promote clearance of a persistent viral infection. Journal of Virology 86:7060—7071.

[28] Amar, J., Burcelin, R., Ruidavets, J.B., Cani, P.D., Fauvel, J., Alessi, M.C., et al., 2008. Energy intake is associated with endotoxemia in apparently healthy men. American Journal of Clinical Nutrition 87:1219—1223.

[29] Grewal, H.M., Karlsen, T.H., Vetvik, H., Ahren, C., Gjessing, H.K., Sommerfelt, H., et al., 2000. Measurement of specific IgA in faecal extracts and intestinal lavage fluid for monitoring of mucosal immune responses. Journal of Immunological Methods 239:53—62.

[30] Abdul-Ghani, M., DeFronzo, R.A., 2007. Fasting hyperglycemia impairs glucose- but not insulin-mediated suppression of glucagon secretion. Journal of Clinical Endocrinology and Metabolism 92:1778—1784.

[31] Hotamisligil, G.S., 2006. Inflammation and metabolic disorders. Nature 444:860—867.

[32] Shoelson, S.E., Lee, J., Goldfine, A.B., 2006. Inflammation and insulin resistance. Journal of Clinical Investigation 116:1793—1801.

[33] Luck, H., Tsai, S., Chung, J., Clemente-Casares, X., Ghazarian, M., Revelo, X.S., et al., 2015. Regulation of obesity-related insulin resistance with gut anti-inflammatory agents. Cell Metabolism 21:527—542.

[34] Moskophidis, D., Lechner, F., Pircher, H., Zinkernagel, R.M., 1993. Virus persistence in acutely infected immunocompetent mice by exhaustion of antiviral cytotoxic effector T cells. Nature 362:758—761.

[35] Fazilleau, N., McHeyzer-Williams, L.J., Rosen, H., McHeyzer-Williams, M.G., 2009. The function of follicular helper T cells is regulated by the strength of T cell antigen receptor binding. Nature Immunology 10:375—384.

[36] Macpherson, A.J., Uhr, T., 2004. Induction of protective IgA by intestinal dendritic cells carrying commensal bacteria. Science 303:1662—1665.

[37] Garrett, W.S., Gallini, C.A., Yatsunenko, T., Michaud, M., DuBois, A., Delaney, M.L., et al., 2010. Enterobacteriaceae act in concert with the gut microbiota to induce spontaneous and maternally transmitted colitis. Cell Host & Microbe 8:292—300.

[38] Koren, O., Spor, A., Felin, J., Fak, F., Stombaugh, J., Tremaroli, V., et al., 2011. Human oral, gut, and plaque microbiota in patients with atherosclerosis. Proceedings of the National Academy of Sciences U S A 108(Suppl. 1):4592—4598.

